Supporting Information

Block Copolymer Micelles Enable Facile Synthesis of Organic-Inorganic Perovskite Nanostructures with Tailored Architecture

Yoonseo Nah,[a] Dohyub Jang[b,c] and Dong Ha Kim*[a,d]

[a] *Division of Chemical Engineering and Materials Science, College of Engineering, Ewha Womans University, 52 Ewhayeodae-gil, Seodaemun-gu, Seoul 03760, Republic of Korea*

[b] *Department of Biomicrosystem Technology, Korea University, 145 Anam-ro, Seongbuk-gu, Seoul 02841, Republic of Korea*

[c] *Center for Theragnosis, Korea Institute of Science and Technology, 5, Hwarang-ro 14-gil, Seongbuk-gu, Seoul 02792, Republic of Korea*

[d] *Department of Chemistry and Nano Science, College of Natural Science, Ewha Womans University, 52 Ewhayeodae-gil, Seodaemun-gu, Seoul 03760, Republic of Korea*

Experimental Details

Materials. Polystyrene-block-poly(2-vinylpyridine) **(**PS-b-P2VP, 34k-b-18k) was purchased from Polymer Source. Lead(II) bromide ($PbBr_2$), methylammonium bromide (MABr), methylammonium chloride (MACl), toluene, methanol (MeOH) were purchased from Sigma Aldrich. All the commercially available chemicals were used as received without further purification.

Synthesis of $PbBr_2$-loaded reverse micelle solution. 87.4 mg of PS-b-P2VP was dissolved in 10 mL toluene under vigorous stirring at 70 ℃ for 3 hr. Excess amounts of $PbBr_2$ powder was added to the micelle solution, and the mixture was stirred vigorously at 70 ℃ for 3 days. Undissolved $PbBr_2$ was removed by centrifugation at 10,000 rpm for 20 min.

Syntheses of $MAPbBr_2X$ nanostructures. MAX (X=Cl, Br) powder was dissolved in 20 μL methanol solution. The above solution was dropped onto the 1 mL $PbBr_2$-loaded reverse micelle solution under various stirring rates at various temperatures.

Inductively coupled plasma mass spectrometer (ICP-MS) measurements. Concentration of dissolved Pb^{2+} ion was measured by using PerkinElmer, NexION300 spectrometer.

Field emission transmission electron microscopy (FE-TEM) measurements. Morphologies of nanostructures were characterized by JEOL, JEM-2100F microscope. Samples were deposited on carbon film coated Cu grid.

Atomic force microscopy (AFM) measurements. Morphologies of the nanostructures were characterized by employing a Bruker, Dimension Edge atomic force microscope. Solution samples were spincoated on Si substrates at 1500 rpm for 45 s.

Optical microscopy measurements. Morphologies of the nanostructures were characterized by using a Nikon, Eclipse LV100D microscope. Solution samples were spincoated on glass substrates at 1500 rpm for 45 s.

Dynamic Light Scattering (DLS) measurements. Hydrodynamic radii of micelles were measured by using Malvern Panalytical, Zetasizer spectrometer at 298 K.

Film X-ray diffraction (XRD) measurements. The crystalline structure of encapsulated nanocrystals was characterized by an EPLEX, SPIN-1200D X-ray diffractometer at 298 K.

Steady-state absorption measurements. UV-vis absorption spectra were obtained using a Varian, Cary 5000 Spectrometer at 298 K. A Hellma quartz cell (beam path length = 1.0 cm) was employed for solution samples.

Steady-state photoluminescence measurements. Steady-state photoluminescence spectra were collected on a JASCO, FP-8500 spectrofluorometer at 298 K. The excitation wavelength was 370 nm. A Hellma quartz cell (beam path length = 1.0 cm) was employed for solution samples. The absolute photoluminescence quantum yield was determined by using an integrating sphere (JASCO). The photon flux of an excitation beam was quantified in the empty sphere, and then both excitation and emission spectra were collected for the two cases: i) sample was directly illuminated by the excitation beam, and ii) sample was indirectly excited by the scattered light. The emission spectra were recorded in the range of 400-700 nm.

Supplementary Figures

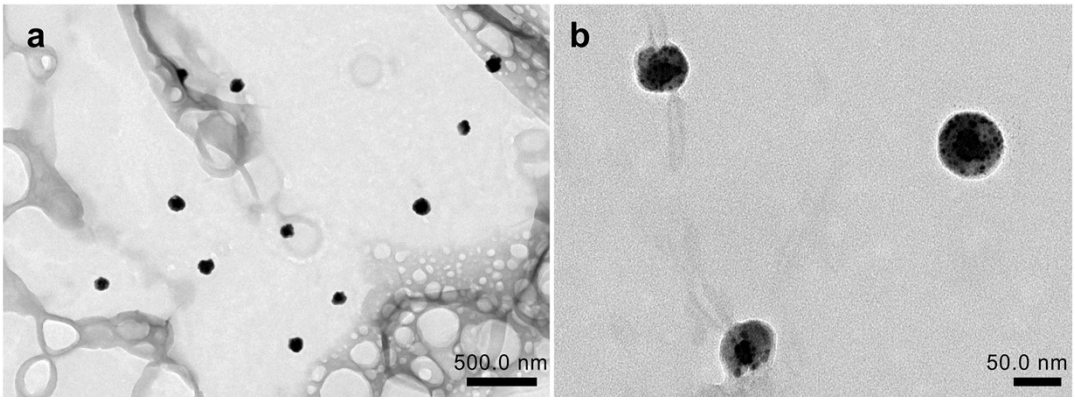

Fig. S1 FE-TEM images of micelles containing $MAPbBr_3$ precursors. The micelle solution was immersed in liquid nitrogen to prevent the crystallization.

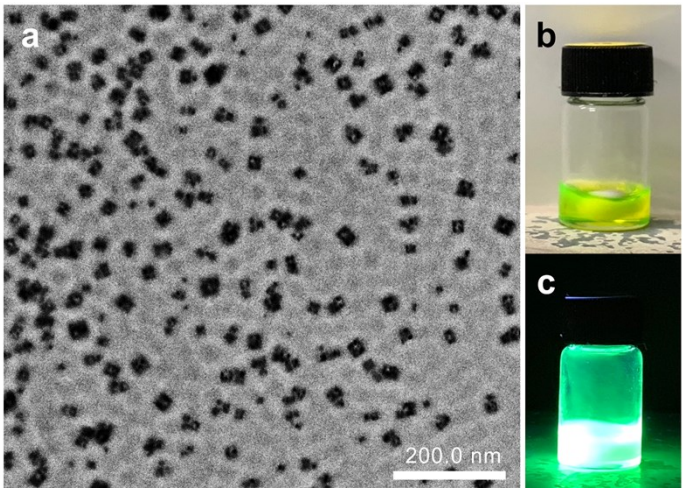

Fig. S2 (a) A FE-TEM image of encapsulated $MAPbBr_3$ nanocrystals and (b, c) photographs of dispersion solution under (b) white light and (c) UV lamp (excitation wavelength = 365 nm).

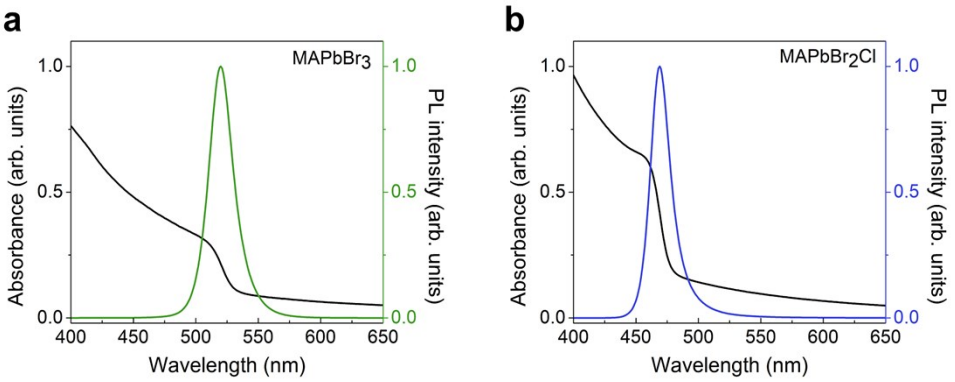

Fig. S3 The steady-state absorption and photoluminescence spectra of encapsulated (a) $MAPbBr_3$ and (b) $MAPbBr_2Cl$ nanocrystals.

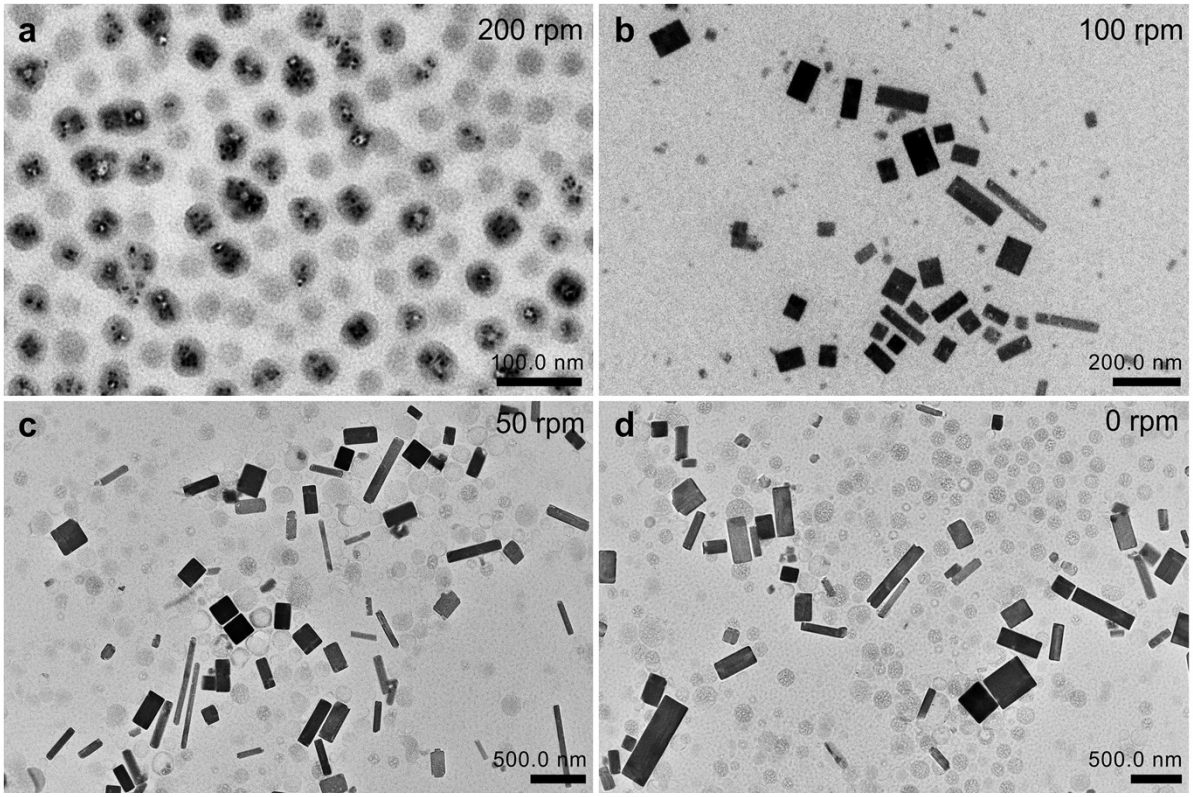

Fig. S4 FE-TEM images of $MAPbBr_3$ nanostructures obtained at 18 ℃ under various stirring rates.

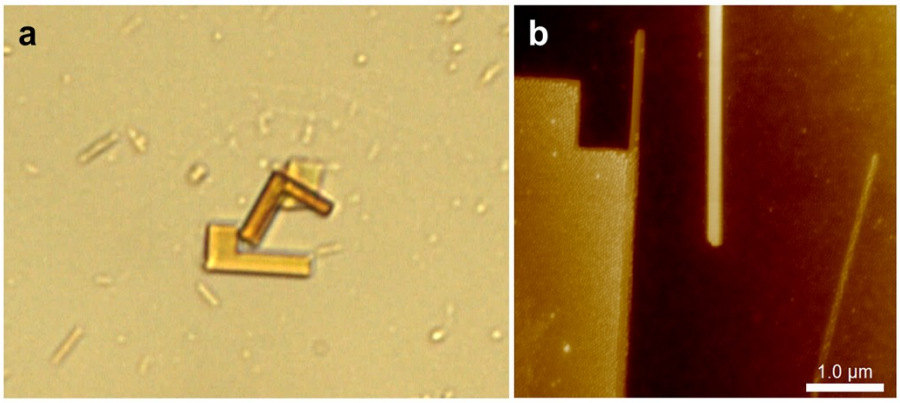

Fig. S5 (a) Optical microscopy image and (b) AFM topography of $MAPbBr_3$ nanostructures exhibiting spiky projections.

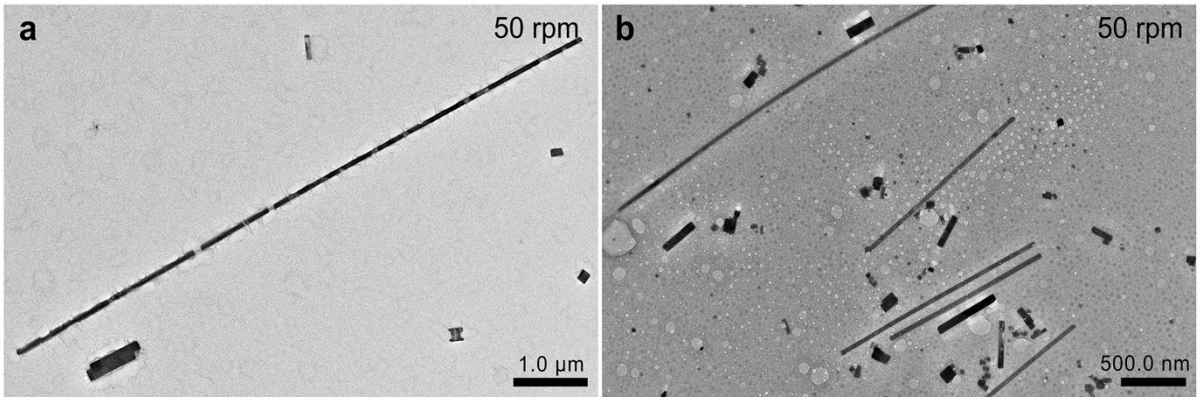

Fig. S6 FE-TEM images of anisotropic $MAPbBr_3$ nanostructures.

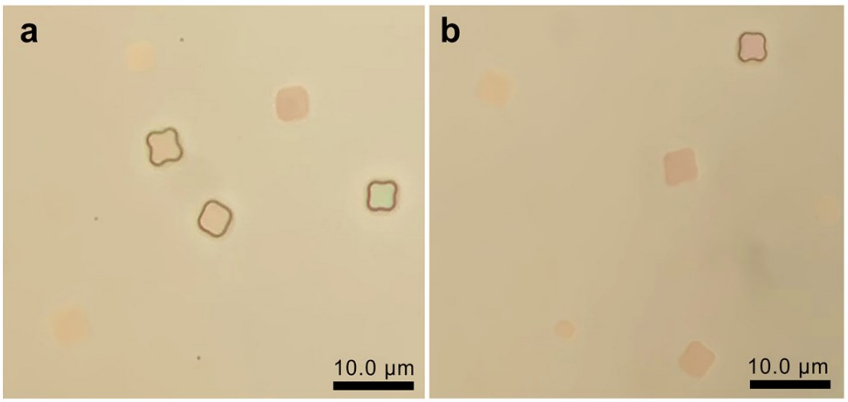

Fig. S7 Optical microscopy images of micron-sized $MAPbBr_3$ nanoplates. The stoichiometric ratio between $PbBr_2$ and MABr was 1:1.